ORIGINAL ARTICLE

Hyperoxia Injury in the Developing Lung Is Mediated by Mesenchymal Expression of Wnt5A

Jennifer M. S. Sucre[1,2], Kasey C. Vickers[3], John T. Benjamin[1], Erin J. Plosa[1], Christopher S. Jetter[1], Alissa Cutrone[4], Meaghan Ransom[5], Zachary Anderson[5], Quanhu Sheng[6], Benjamin A. Fensterheim[4], Namasivayam Ambalavanan[7], Bryan Millis[2,8], Ethan Lee[2], Andries Zijlstra[9], Melanie Königshoff[10], Timothy S. Blackwell[2,11,12], and Susan H. Guttentag[1]

[1]Mildred Stahlman Division of Neonatology, Department of Pediatrics, [2]Department of Cell and Developmental Biology, and [8]Cell Imaging Shared Resource, Vanderbilt University, Nashville, Tennessee; [3]Division of Cardiovascular Medicine, Department of Medicine, [5]Department of Pediatrics, [6]Department of Biostatistics, [9]Department of Pathology, Microbiology, and Immunology, and [11]Division of Allergy, Pulmonary and Critical Care Medicine, Department of Medicine, Vanderbilt University Medical Center, Nashville, Tennessee; [4]Medical Scientist Training Program, Vanderbilt University School of Medicine, Nashville, Tennessee; [7]Division of Neonatology, Department of Pediatrics, University of Alabama at Birmingham, Birmingham, Alabama; [10]Division of Pulmonary Sciences and Critical Care Medicine, Department of Medicine, University of Colorado, Denver, Colorado; and [12]Nashville Veterans Affairs Medical Center, Nashville, Tennessee

ORCID IDs: 0000-0002-6613-1439 (J.M.S.S.); 0000-0001-9414-5128 (M.K.); 0000-0003-4420-5879 (S.H.G.).

Abstract

Rationale: Bronchopulmonary dysplasia (BPD) is a leading complication of preterm birth that affects infants born in the saccular stage of lung development at <32 weeks of gestation. Although the mechanisms driving BPD remain uncertain, exposure to hyperoxia is thought to contribute to disease pathogenesis.

Objectives: To determine the effects of hyperoxia on epithelial–mesenchymal interactions and to define the mediators of activated Wnt/β-catenin signaling after hyperoxia injury.

Methods: Three hyperoxia models were used: A three-dimensional organotypic coculture using primary human lung cells, precision-cut lung slices (PCLS), and a murine *in vivo* hyperoxia model. Comparisons of normoxia- and hyperoxia-exposed samples were made by real-time quantitative PCR, RNA *in situ* hybridization, quantitative confocal microscopy, and lung morphometry.

Measurements and Main Results: Examination of an array of Wnt ligands in the three-dimensional organotypic coculture revealed increased mesenchymal expression of *WNT5A*. Inhibition of Wnt5A abrogated the BPD transcriptomic phenotype induced by hyperoxia. In the PCLS model, Wnt5A inhibition improved alveolarization following hyperoxia exposure, and treatment with recombinant Wnt5a reproduced features of the BPD phenotype in PCLS cultured in normoxic conditions. Chemical inhibition of NF-κB with BAY11–7082 reduced *Wnt5a* expression in the PCLS hyperoxia model and *in vivo* mouse hyperoxia model, with improved alveolarization in the PCLS model.

Conclusions: Increased mesenchymal Wnt5A during saccular-stage hyperoxia injury contributes to the impaired alveolarization and septal thickening observed in BPD. Precise targeting of Wnt5A may represent a potential therapeutic strategy for the treatment of BPD.

Keywords: bronchopulmonary dysplasia; Wnt; lung injury; hyperoxia

(Received in original form August 2, 2019; accepted in final form February 4, 2020)

This work was supported by K08HL143051(J.M.S.S.), R01CA218526 (A.Z.), NIH GM108807 (S.H.G.), U01-HL101794 (J.T.B.), U01 HL122626 (N.A.), R01 HL129907 (N.A.), U01 HL 133,536 (N.A.), P01HL92870 (T.S.B.), R01HL085317 (T.S.B.), R01HL128996 (K.C.V.), R01HL127173 (K.C.V.), P01HL116263 (K.C.V.), R35GM122516 (E.L.), 1R01HL141380 (M.K.), Department of Veterans Affairs (T.S.B.), Francis Family Foundation (J.M.S.S.), and the Julia Carell Stadler Chair in Pediatrics (S.H.G.).

Author Contributions: Conception and design: J.M.S.S., K.C.V., J.T.B., E.J.P., C.S.J., N.A., E.L., A.Z., M.K., T.S.B., and S.H.G. Performing experiments: J.M.S.S., J.T.B., C.S.J., A.C., M.R., Z.A., and B.A.F. Analysis and interpretation: J.M.S.S., K.C.V., Q.S., B.A.F., B.M., E.L., A.Z., T.S.B., and S.H.G. Drafting the manuscript: J.M.S.S. and S.H.G. Editing manuscript: J.M.S.S., K.C.V., J.T.B., E.J.P., C.S.J., A.C., M.R., Z.A., Q.S., B.A.F., N.A., B.M., E.L., A.Z., M.K., T.S.B., and S.H.G.

Correspondence and requests for reprints should be addressed to Jennifer M. S. Sucre, M.D., Vanderbilt University, 2215B Garland Avenue, 1125 Light Hall, Nashville, TN 37232. E-mail: jennifer.sucre@vanderbilt.edu.

This article has a related editorial.

This article has an online supplement, which is accessible from this issue's table of contents at www.atsjournals.org.

Am J Respir Crit Care Med Vol 201, Iss 10, pp 1249–1262, May 15, 2020

Originally Published in Press as DOI: 10.1164/rccm.201908-1513OC on February 5, 2020
Internet address: www.atsjournals.org

At a Glance Commentary

Scientific Knowledge on the Subject: While the environmental triggers associated with bronchopulmonary dysplasia (BPD) have been described, the precise molecular mechanisms driving the pathophysiology of BPD remain elusive.

What This Study Adds to the Field: This study identifies mesenchymal expression of Wnt5A as a driver of the impaired lung development seen after hyperoxia injury and defines a potential mechanistic link between hyperoxia injury and aberrant expression of Wnt5A. Further, we explore precise manipulation of Wnt5A as a target for future therapeutic investigation in the treatment of BPD.

Bronchopulmonary dysplasia (BPD) is a leading complication in survivors of preterm birth and a major comorbidity associated with neurodevelopmental disability in preterm infants. BPD is thought to result from injury to vulnerable saccular-stage lung (23–32 wk gestation) and results in pulmonary insufficiency, with characteristic histopathology of arrested alveolarization and interstitial fibrosis in its most severe forms (1). Although multiple environmental insults, including hyperoxia, have been shown to play a role in BPD pathogenesis (2), the precise molecular mechanisms that mediate BPD after lung injury remain elusive.

Precisely coordinated activation of the Wnt/β-catenin signaling pathway is essential for normal lung development (3, 4), and dysregulated Wnt signaling is emerging as a mediator of chronic lung disease across the lifespan, with Wnt signaling implicated in chronic lung diseases such as BPD and idiopathic pulmonary fibrosis (5). We have previously demonstrated a pattern of aberrantly activated β-catenin in human BPD tissue and in hyperoxia models of BPD (6, 7); however, the specific mediators that respond to hyperoxia and drive increased signaling in Wnt pathway in the developing lung have not been defined.

To study hyperoxia injury in the developing lung, we previously developed a novel three-dimensional organotypic coculture (3D-OTC) system that allows for examination of the interactions between primary alveolar type 2 (AT2) cells and fibroblasts (8). This model, along with an *ex vivo* precision-cut lung slices (PCLS) model of alveolarization and an *in vivo* mouse model of postnatal hyperoxia exposure, was used to investigate drivers of dysregulated Wnt signaling after injury, specifically increased mesenchymal expression of Wnt5A. Although the abnormal lung development after saccular-stage injury is likely caused by multiple factors and pathways, this work identifies a mechanistic link between hyperoxia injury and increased expression of Wnt5A and explores precise manipulation of Wnt5A as a target for future therapeutic investigation.

Some of the results of these studies have been previously reported in the form of an abstract (9).

Methods

Primary Epithelial Cell Isolation

Second-trimester human lung tissues (15–20 wk gestation) were isolated as previously published (10, 11) in accordance with protocols approved by the Vanderbilt University Institutional Review Board and in compliance with NIH Guidelines for Human Stem Cell Research. The isolated epithelial cells were cultured in Waymouth's medium supplemented with 10 nM dexamethasone, 0.1 nM 8-bromo-cyclic-AMP, and 0.1 mM isobutylmethylxanthine, (referred to as DCI), which has been demonstrated to promote differentiation and maturation of AT2 cells (11, 12).

Isolation of Primary Human Lung Fibroblasts

Using the same second-trimester fetal lung tissues described above, fetal lung fibroblasts were isolated, and cells between passages 5 and 15 were used for experiments, with additional details about isolation in the online supplement.

In Vitro NF-κB Inhibition

Transgenic mice that express a *Myc*-His-tagged mutant avian IκBα (NF-κB [nuclear factor-κB] inhibitor) under control of seven repeats of the tetracycline operator-minimal cytomegalovirus promoter (13) were crossed with homozygous Rosa-rtTA (Rosa-reverse tetracycline transactivator) mice that express the reverse tetracycline transactivator under control of the ubiquitous ROSA26 promoter. Double-transgenic pups derived from this crossing express both the tet-O7-IκBα-DN-*Myc*-His construct and reverse transactivator in every cell. At postnatal day 2 (P2), saccular-stage lung fibroblasts were isolated from these pups as previously described (14). At passage 4, fibroblasts in culture were treated with doxycycline to induce transgene activation and expression of IκBα.

Cell culture. Additional details about cell culture conditions and mouse lung epithelium (MLE-15) cell line are available in the online supplement.

Assembly and Culture of 3D-OTCs

As previously described (8), 3D-OTCs were assembled on 24-mm transwells and processed for histology and RNA isolation. Cocultures may contain fibroblasts and epithelial cells from different primary tissues. OTCs were exposed to hyperoxia (70%) in a HeraCell 150i incubator for 48 hours and compared with normoxia-cultured controls (5% oxygen, which produces a P_{O_2} of 60–70 mm Hg in growth media and mimics physiologic oxygen tension [15]).

Transcriptomics

Total RNA was isolated using RNEasy kits (Qiagen) and reverse-transcribed using SuperScript variable input linear output complementary DNA synthesis kit (Invitrogen). Wnt pathway array (Thermo Fisher) was used to determine the relative expression of Wnt ligands. Real-time quantitative PCR (qPCR) was used to confirm expression of genes, with specific TaqMan probes in the online supplement.

Animal Care, Hyperoxia Experiments, and Tissue Fixation

C57BL/6 mice were exposed to 85% O_2 (hyperoxia) or 21% O_2 normoxia conditions from P2 until 14 days of age (P14), as described previously (16, 17). For experiments in which chemical inhibition of NF-κB signaling was used, pups received intraperitoneal injections of BAY11–7082 (Sigma) (10 mg/kg) or saline control on P12–13 as described previously (18). On P14, lungs were inflation-fixed by gravity filling with 10% buffered formalin and paraffin embedded. This protocol was approved by the Institutional Animal Care and Use Committees of University of

Alabama at Birmingham and Vanderbilt University and was in compliance with the Public Health Services policy on humane care and use of laboratory animals.

PCLS

PCLS 300 μm in thickness were made from the lungs of mouse pups on P4–7 using previously published methods (19, 20), with additional details in the online supplement. Slices were cultured in Dulbecco's modified Eagle medium:F12 for 96 hours in either hyperoxia (70% O_2) or normoxia culture conditions (5% O_2) in the HeraCell 150i incubator. Neutralizing antibodies against Wnt5A (MAB645, R&D Systems), recombinant Wnt5A (Time Bioscience), and NF-κB inhibitor BAY11–7082 (Sigma) were added to cell culture media as described in the RESULTS section. Neutralizing capacity of anti-Wnt5A antibody has been previously validated (21).

Immunofluorescence

Immunofluorescence (IF) was performed as described previously (7, 22, 23), with additional details about specific antibodies in the online supplement.

RNA *In Situ* Hybridization

RNAScope technology (ACDBio) was used to perform all RNA *in situ* hybridization (RNA ISH) experiments (24) according to manufacturer's instructions, with specific probe details in the online supplement.

Confocal Microscopy

IF images were acquired using an automated TiE inverted fluorescence microscope platform equipped with an encoded motorized stage and Plan Apo 60 × 1.40 numerical aperture objective (Nikon Instruments, Inc.), with additional details in the online supplement. NIS-Elements software (Nikon Instruments, Inc.) was utilized for both acquisition and image analysis. To enumerate the number of RNAscope puncta, a custom automated script was performed within NIS-Elements and applied in batch so as to treat all images equally. Full details of this script are in the online supplement.

Lung Morphometry

Formalin-fixed, paraffin-embedded sections of the PCLS were stained with hematoxylin and eosin as previously described (25). Lung morphometry, including mean linear intercept (MLI) and airspace volume density, was performed on images acquired via a 40× objective for six sections per lung slice, with a minimum of $n = 4$ mice in each group, as previously described (25), using ImageJ software to calculate MLI and airspace volume density.

Multiplex Cytokine Array

Cytokine/chemokine Magnetic Bead 32-Multiplex Panel (MCYTMAG-70K-PX32; Millipore) was performed on PCLS-conditioned media after 96 hours exposure to either hyperoxia or normoxia conditions in triplicate per manufacturer's instructions. The Multiplex assay was read on the Luminex MAGPIX platform available in the Vanderbilt Hormone and Analytical Services Core Facility.

Statistics

Except as indicated, experiments were performed a minimum of three times, with triplicate values used in qPCR experiments. Except where indicated in figure legends, all values are reported as mean values ± SD. Statistical analyses were performed using GraphPad Prism (version 7). Two-tailed Welch's *t* test was used for two-group comparisons, with Holm-Sidak correction for multiple comparisons. Two-way ANOVA was used for comparisons between multiple groups, with the Tukey method to correct for multiple comparisons. An adjusted P value < 0.05 was considered statistically significant.

Results

Exposed to Hyperoxia, 3D-OTC Demonstrate Significant Transcriptomic Changes Mediated by Mesenchymal Expression of Wnt5A

Compared with 3D-OTC maintained in normoxic conditions, exposure of 3D-OTC to 70% O_2 (hyperoxia) for 48 hours resulted in increased expression of genes associated with fibrosis and BPD, including *ACTA2* (α-smooth muscle actin), *COL1A1*(collagen 1), and *ELN* (elastin) (Figure 1A), as well as increased expression of α-SMA (α-smooth muscle actin) localized to the mesenchymal cells (Figure 1B). In addition, we found that hyperoxia exposure of the 3D-OTCs resulted in decreased expression of cell-cycle genes previously identified as associated with alveologenesis and lung branching (6), including *FOXM1* (forkhead box M1), *MYB* (a transcription factor and oncogene named for avian myeloblastosis virus [26]), *MCM2* (minichromosome maintenance complex component 2), and *MCM3* (minichromosome maintenance complex component 3) (4, 27–29) (Figure 1C). IF for FOXM1 confirmed decreased nuclear localization under hyperoxia conditions (Figure 1D). Despite these changes in gene expression and cellular phenotype, hematoxylin and eosin staining showed similar histology of the 3D-OTC between these groups, and no differences in cell proliferation (by Ki67 staining) were identified (Figures 1E and 1F). Terminal deoxynucleotide transferase–mediated dUTP nick end label (TUNEL) staining showed very few apoptotic cells in both groups (Figure E1A in the online supplement). Of note, we saw no significant change in expression of *FGF18,* a gene associated with airway branching and septation (Figure E2). This pattern of increased expression of fibrotic genes and decreased expression of genes associated with alveologenesis in this 3D-OTC hyperoxia model mimics the BPD phenotype of impaired alveolarization and fibrosis seen in other models of BPD (16, 30).

Because prior studies have suggested that hyperoxia injury results in increased Wnt signaling, and evidence of activated Wnt/β-catenin signaling (increased *AXIN2* expression and nuclear accumulation of β-catenin) has been found in human BPD tissue (6), we were interested in determining whether active Wnt signaling was present in our hyperoxia injury model. We found increased nuclear accumulation of p-β-catenin^{Y489} (β-catenin phosphorylated at tyrosine-489) in cells positive for SP-B (surfactant protein-B), suggesting that the 3D-OTC hyperoxia model replicates activated Wnt/β-catenin signaling previously observed in AT2 cells in human BPD tissue and in mouse models of BPD (6, 7) (Figure 2A). In addition, we detected increased expression of the Wnt target gene *AXIN2* by RNA ISH in both AT2 cells and fibroblasts (Figures 2B and 2D) and by real-time qPCR (Figure 2C) in hyperoxia-exposed 3D-OTC, indicating that the canonical Wnt pathway is activated in response to hyperoxia exposure. Because of difficulty in separating mesenchymal cells from epithelial cells in the 3D-OTC for RNA isolation, we made 3D-OTC models with human fibroblasts in the matrix layer and mouse MLE-15 cells, a mouse epithelial cell line that has been shown to have

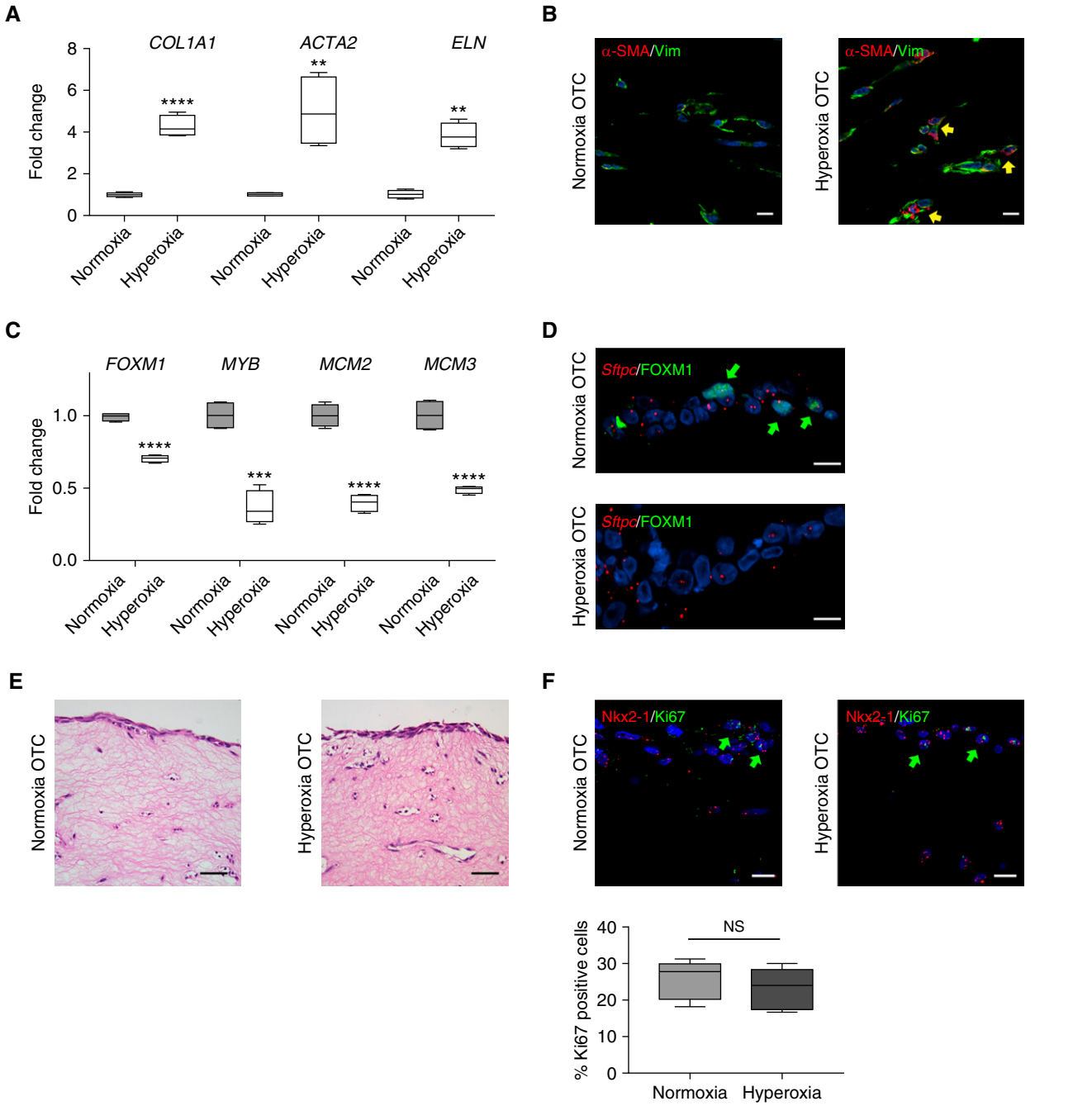

Figure 1. Three-dimensional organotypic cocultures (3D-OTC) replicate the bronchopulmonary dysplasia transcriptomic phenotype. (*A*) With hyperoxia exposure, 3D-OTC comprised of primary fetal lung mesenchymal cells and type 2 alveolar epithelial cells have increased expression of genes associated with fibrosis with hyperoxia exposure, shown as mean ± SD. $^{**}P < 0.01$ and $^{****}P < 0.0001$. (*B*) Immunofluorescence (IF) shows increased α-SMA (α-smooth muscle actin) (red) in fibroblasts stained for vimentin (Vim) (green) in hyperoxia 3D-OTC (yellow arrows indicate double-positive cells). Scale bars, 10 μm. (*C*) With hyperoxia exposure, 3D-OTC have decreased expression of genes associated with alveolarization when compared with normoxia-cultured controls, shown as mean ± SD. $^{***}P < 0.001$ and $^{****}P < 0.0001$. (*D*) IF for FOXM1 (green) and RNA *in situ* hybridization for SPC gene *Sftpc* showed decreased nuclear FOXM1 in hyperoxia 3D-OTC (green arrows indicate FOXM1$^+$ nuclei). Scale bars, 10 μm. (*E*) Hematoxylin and eosin staining of 3D-OTC cultured in normoxia and hyperoxia. Scale bars, 25 μm. (*F*) IF for mitotic marker Ki67 (green) and epithelial marker Nkx2.1 (red) shows no significant difference in proliferation between 3D-OTCs cultured in normoxia and hyperoxia, with quantification expressed as percent Ki67-positive cells and determined by counting 36 high-powered fields per group (green arrows indicate Ki67$^+$ cells). $N = 5$ biological replicates, with 3 technical replicates used for each sample. NS = nonsignificant.

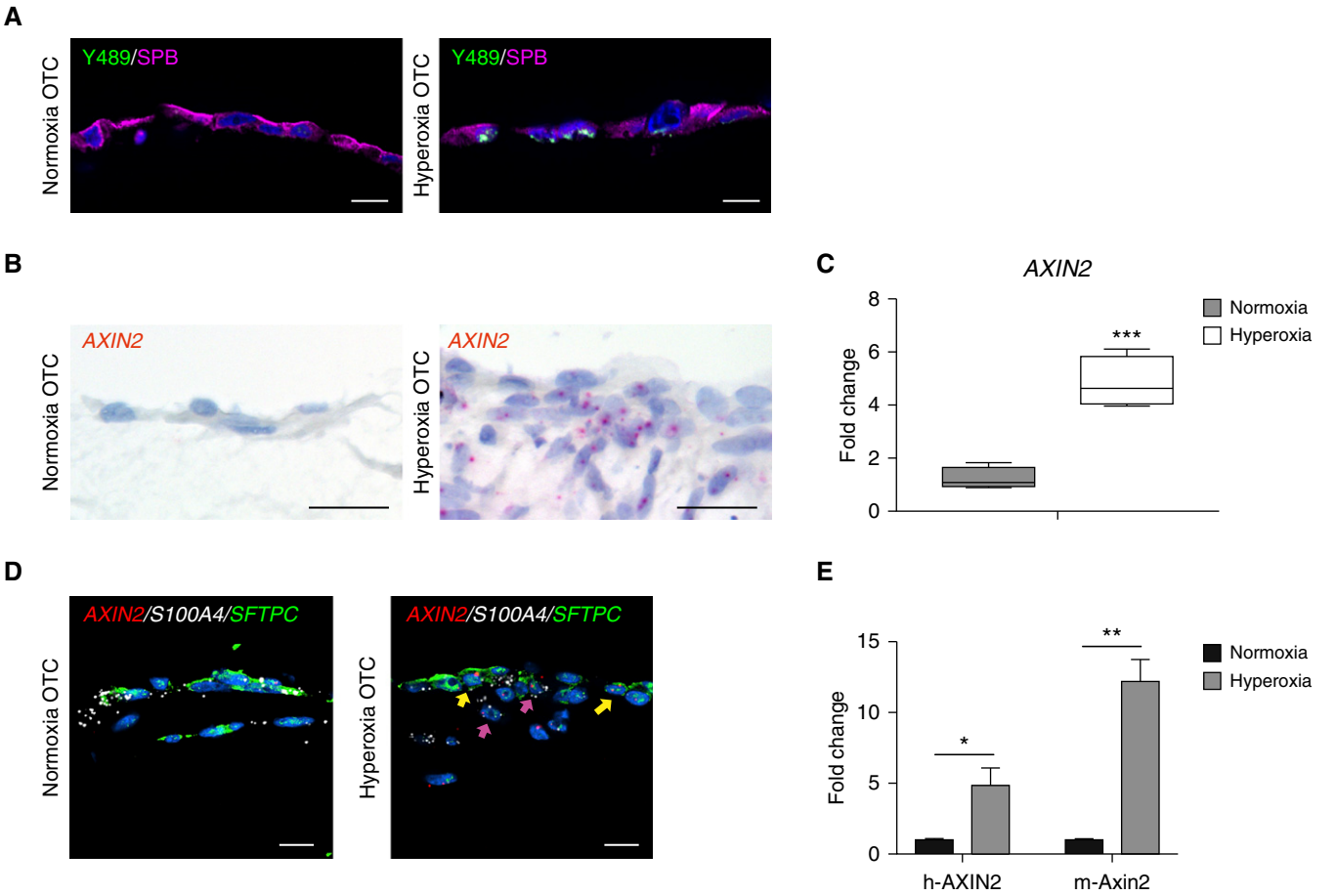

Figure 2. Hyperoxia exposure of three-dimensional organotypic cocultures (3D-OTC) stimulates active Wnt/β-catenin signaling. (*A*) Immunofluorescence for p-β-catenin^{Y489} (nuclear β-catenin phosphorylated at tyrosine-489) (green), an established marker of Wnt activation, and SPB (surfactant protein-B) (purple) shows increased nuclear p-β-catenin^{Y489} in hyperoxia-exposed OTC when compared with normoxic-cultured controls. Scale bars, 10 μm. (*B*) RNA *in situ* hybridization (RNA ISH) shows increased expression of Wnt target gene *AXIN2* with hyperoxia exposure. Scale bars, 10 μm. (*C*) Real-time quantitative PCR (qPCR) comparing hyperoxia-exposed 3D-OTC with normoxia-cultured OTC shows increased expression of *AXIN2*. $^{***}P < 0.01$. (*D*) Multiplex RNA ISH showing increased expression of *AXIN2* (red) in hyperoxia 3D-OTC relative to normoxia controls. *AXIN2* is expressed in epithelial cells coexpressing *SFTPC* in green (yellow arrows) and mesenchymal cells expressing fibroblast marker *S100A4* in white (magenta arrows). Scale bars, 10 μm. (*E*) MLE-15 cells were combined with human lung fibroblasts to make 3D-OTC, which were exposed to hyperoxia. Real-time quantitative PCR was performed with species-specific probes for *AXIN2/Axin2*. $^{*}P < 0.05$ and $^{**}P < 0.01$. Data are representative of three biological replicates for each condition, with three technical replicates for each sample used for qPCR.

properties of AT2 cells (31). Species-specific probes showed there was both human and mouse expression of Wnt target gene *Axin2/AXIN2* by real-time qPCR (Figure 2D), indicating that activated Wnt/β-catenin signaling was present in both cell types.

To identify which Wnt ligands were driving increased Wnt signaling after hyperoxia exposure, we employed a Wnt pathway qPCR array and discovered increased expression of *WNT2B, WNT5A, WNT9A,* and *WNT16* (Figure 3A). Because increased expression of Wnt5A has been previously associated with other chronic lung diseases, including idiopathic pulmonary fibrosis (21) and chronic obstructive pulmonary disease (32), we pursued Wnt5A further as a potential driver of the hyperoxia injury response. We confirmed that hyperoxia increased expression of *WNT5A* mRNA in our 3D-OTC model by real-time qPCR (Figure 3B) and RNA ISH (Figures 3C and 3D). With multiplex RNA ISH, we found that cells expressing a fibroblast marker *S100A4* (S100 calcium-binding protein A4) coexpressed *WNT5A* (Figure 3D), suggesting that mesenchymal cells were the source of the increased *WNT5A* expression. This was confirmed with MLE-15/human fibroblast 3D-OTCs, which demonstrated expression of only human, but not mouse, *WNT5A*, further supporting the conclusion that WNT5A is restricted to the mesenchymal component of the coculture 3D-OTC model (Figure 3E).

To test whether Wnt5A promotes the BPD transcriptomic phenotype identified in 3D-OTC after hyperoxia exposure, we added recombinant Wnt5A protein (33) to normoxia-cultured 3D-OTC and identified increased expression of profibrotic genes, *ACTA2* and *COL1A1,* and decreased expression of cell-cycle genes *FOXM1* and *MCM2* (Figure 3F), similar to hyperoxia (Figure 3F). Wnt5A did not alter expression of *MYB*, *ELN*, or *MCM3* under normoxic

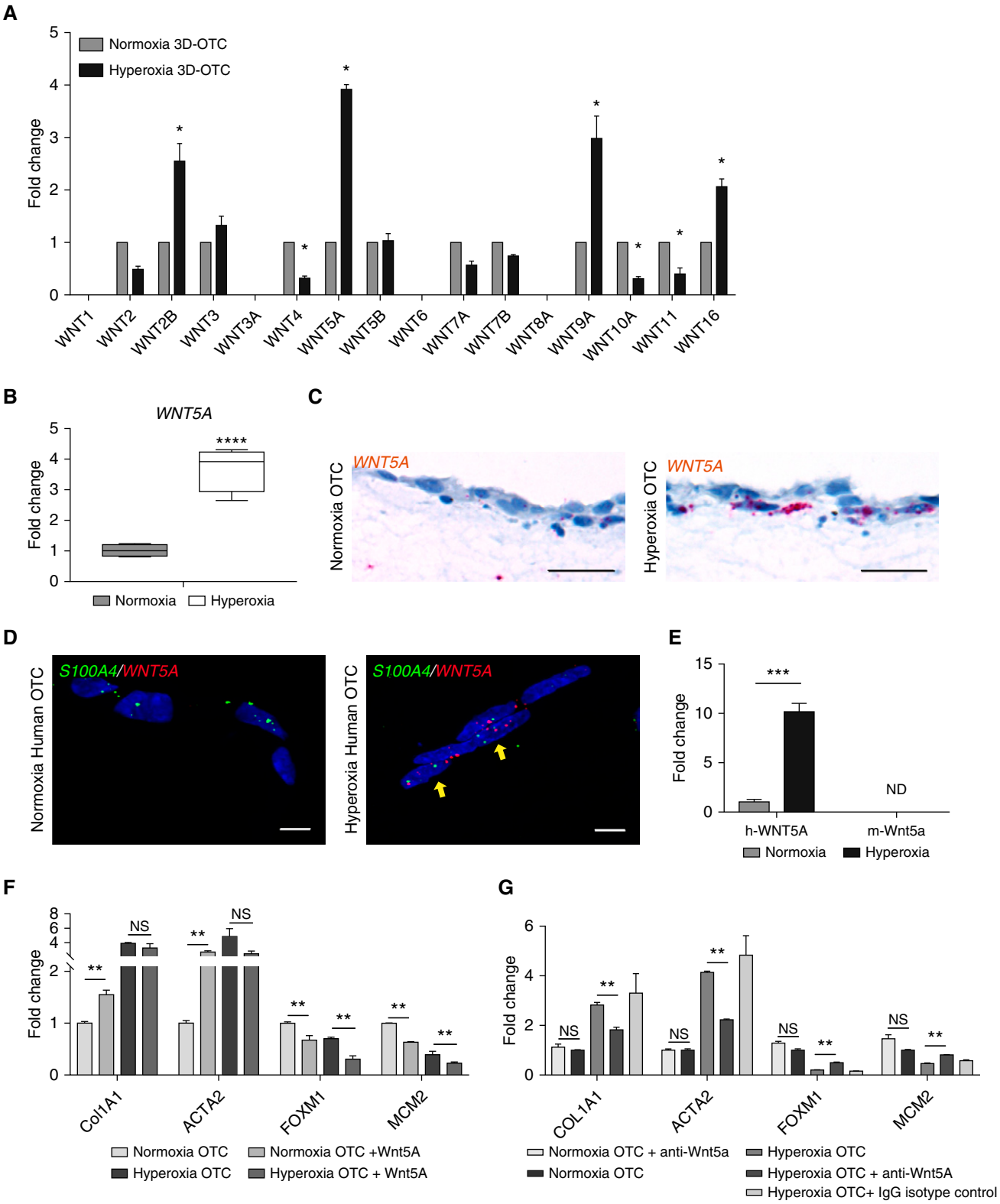

Figure 3. Hyperoxia exposure of three-dimensional organotypic cocultures (3D-OTC) results in mesenchymal expression of Wnt5A. (*A*) Wnt pathway array shows relative expression of Wnt ligands in 3D-OTC cultured in hyperoxia and normoxia conditions, normalized to normoxia. Expression was considered to be 0 if cycle threshold value was >35. *$P < 0.001$. (*B*) Confirmation of increased expression of *WNT5A* by quantitative PCR (qPCR) with TaqMan probes. ****$P < 0.001$. (*C*) RNA *in situ* hybridization demonstrating increased expression of *WNT5A* (red) with hyperoxia exposure. Scale bars, 10 μm. (*D*) Multiplex RNA *in situ* hybridization shows coexpression of *WNT5A* (red) by mesenchymal cells expressing fibroblast marker *S100A4* (green), with yellow

conditions (Figure E3A). In contrast, addition of Wnt5A neutralizing antibody to hyperoxia-exposed 3D-OTC models resulted in decreased expression of *ACTA2* and *COL1A1* and increased expression of *FOXM1* and *MCM2* (Figure 3G), with no significant differences noted in *ELN*, *MYB*, or *MCM3* expression (Figure E3B). Together, these data suggest that Wnt5A mediates an important component of the transcriptomic response to hyperoxia injury in our 3D-OTC model.

Impaired Alveolarization in Hyperoxia Is Attenuated with Wnt5A Neutralization

To study the effects of hyperoxia and increased Wnt5A activity on alveolarization, we cultured PCLS (19) from P4 to P7 mouse pups in hyperoxia (70% oxygen) or normoxia for 96 hours. Hyperoxia-exposed PCLS exhibited a striking phenotype of increased septal thickness as quantified by airspace volume density (25) and decreased alveologenesis as measured by MLI (Figures 4A–4C). Analysis of conditioned media from hyperoxia-exposed PCLS with a multiplex cytokine array identified a significant increase in the following NF-κB–dependent cytokines with hyperoxia: VEGF (vascular endothelial growth factor), LIF (leukemia inhibitory factor), KC (keratin chemoattractant), and IL-6 (Figure E4).

In hyperoxia-exposed PCLS, addition of anti-Wnt5A neutralizing antibodies rescued the alveolarization defect (Figure 4A). In contrast, the addition of recombinant Wnt5A induced *ex vivo* impaired alveolarization under normoxia conditions (Figures 4A and 4C). MLI was unchanged in normoxia-cultured PCLS treated with anti-Wnt5a neutralizing antibodies, and the addition of IgG isotype control did not affect the phenotype in normoxia or hyperoxia PCLS (Figures 4A and 4C). In PCLS cultured in hyperoxia, cellular proliferation was increased as indicated by increased $Ki67^+$ cells, some of which were also positive for AT2 marker Nkx2.1 (Figure 4D); however, addition of anti-Wnt5A antibodies or recombinant Wnt5A did not alter proliferation in either normoxia or hyperoxia (Figure E2A). TUNEL+ cells were rare in all culture conditions (Figure E1). These findings from the *ex vivo* model of hyperoxia injury support the conclusion that impaired alveolarization is driven, in part, by *Wnt5A* expression in response to hyperoxic injury.

To validate the finding of increased *Wnt5a* expression associated with hyperoxia exposure *in vivo*, we utilized a neonatal hyperoxia injury model (16, 34). As previously described, pups exposed to 85% oxygen over 14 days developed a BPD-like phenotype characterized by impaired alveolarization and septal thickening (Figure 5A) (17, 35). Hyperoxia-exposed mouse lungs exhibited expression of *Wnt5a* by RNA ISH only in cells coexpressing *S100a4* (Figure 5B), whereas expression of the Wnt target gene *Axin2* was also observed to be localized in cells expressing *Wnt5a,* as well as cells coexpressing *Sftpc* (surfactant protein-c) (Figure 5C). Quantification of RNA ISH signal showed significantly increased expression of both *Wnt5a* and *Axin2* mRNA levels when compared with normoxia-exposed mouse lungs (Figure 5D).

RNA ISH of lung sections collected from human infants who died with BPD demonstrated a pattern of increased expression of *WNT5A* and coexpression with *S100A4* that was not demonstrated in infants who died of nonrespiratory causes (Figure 6A), with quantitative image analysis confirming increased expression of *WNT5A* in infants with BPD (Figure 6B). Increased *AXIN2* expression has been previously reported in BPD tissue (7), and multiplex RNA ISH confirmed *AXIN2* expression in both AT2 cells and fibroblasts (Figure 6C). Together these data suggest that the finding of increased Wnt5A expression with hyperoxia injury in our *in vitro, ex vivo, and in vivo* models has relevance in our understanding of BPD.

Wnt5a Expression in the Setting of Hyperoxia Injury Is Mediated by NF-κB in the Developing Lung

Because we identified increased expression of NF-κB–dependent cytokines in our hyperoxia-exposed PCLS model, and previous work in murine and human *in vitro* systems has identified putative NF-κB transcription factor binding sites within the Wnt5a promoter (36, 37), we investigated whether NF-κB contributes to Wnt5A induction in hyperoxia injury. We exposed P4–7 PCLS to hyperoxia in the presence and absence of a specific inhibitor of NF-κB signaling, BAY11–7082 (100 μM), which inhibits IκBα (nuclear factor of kappa light polypeptide gene enhancer in B-cells inhibitor, α) phosphorylation (38, 39). Hyperoxia-exposed PCLS cultured in the presence of the NF-κB inhibitor over 96 hours exhibited decreased *Wnt5a* mRNA expression and decreased production of NF-κB–dependent cytokines when compared with hyperoxia alone (Figures 7A and 7B and E5A) by RNA ISH, quantitative image analysis, and cytokine array. By histology, we found that hyperoxia-exposed PCLS treated with the NF-κB inhibitor had an MLI and septal thickness (as quantified by airspace volume density) that was similar to the MLI of normoxia-cultured PCLS (Figures 7C–7E). In contrast, there was no change in *Wnt5a* expression or MLI in normoxia-cultured PCLS exposed to BAY11–7082 (Figures E5A and 7A–7D). To validate the connection between NF-κB and *Wnt5A* expression *in vivo,* hyperoxia-exposed pups were administered BAY11–7082 on P12–13, which resulted in decreased *Wnt5a* expression in the lungs when compared with hyperoxia exposure

Figure 3. (*Continued*). arrows indicating cells coexpressing both genes. Scale bars, 10 μm. (*E*) MLE-15 cells were combined with human lung fibroblasts to make 3D-OTC, which were exposed to hyperoxia. Real-time quantitative PCR was performed with species-specific probes, with only increased expression of human *WNT5A*. Cycle threshold was >35. ***$P < 0.001$. (*F*) Addition of rWnt5A (recombinant Wnt5A) protein to OTC partially replicates the transcriptomic response to hyperoxia, with significantly increased expression of *COL1A1* and *ACTA2*, with decreased expression of *FOXM1* and *MCM2* in normoxia. Addition of rWNT5a had no significant effect of the expression of *MYB*, *ELN,* and *MCM3*. Added rWnt5A to hyperoxia 3D-OTC further decreased expression of *FOXM1* and *MCM2*. **$P < 0.01$. (*G*) Treatment of hyperoxia-exposed cocultures with anti-Wnt5A neutralizing antibody (aWnt5A) during hyperoxia exposure partially attenuated the transcriptomic response to hyperoxia, with decreased expression of *ACTA2*, *COL1A1*, and increased expression of alveologenesis-associated genes *FOXM1* and *MCM2*. There were no significant differences between hyperoxia-exposed OTC and hyperoxia-exposed OTC treated with IgG isotype control antibody, or between normoxia OTC and normoxia OTC exposed to aWnt5A. **$P < 0.01$. Data are representative of three biological replicates for each condition, with three technical replicates for each sample used for qPCR. ND = not detected; NS = nonsignificant.

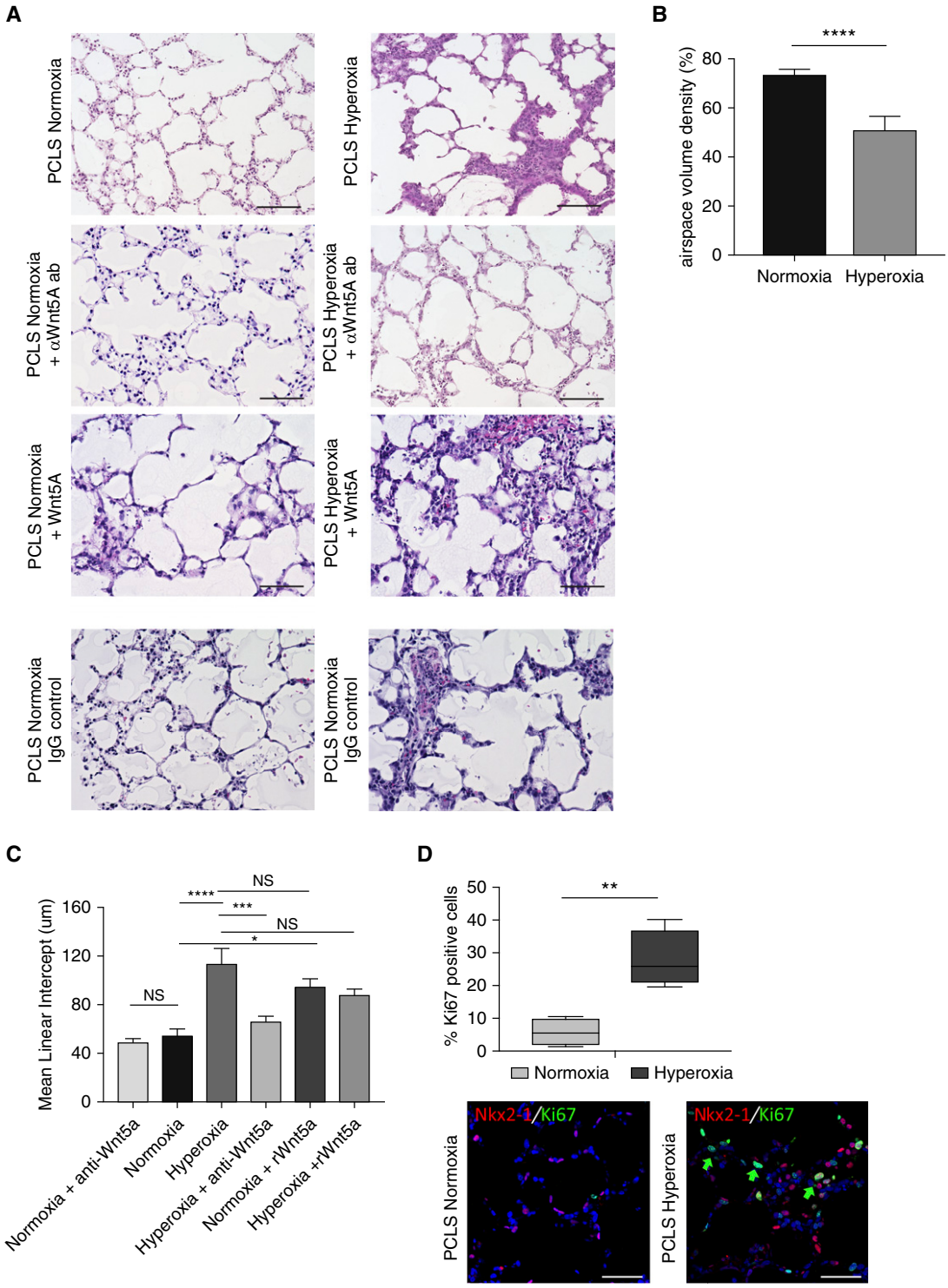

Figure 4. Wnt5A mediates septal thickening and impaired alveolarization observed in hyperoxia exposure. (*A*) Hematoxylin and eosin staining of precision-cut lung slices (PCLS) from PN4 mouse exposed to normoxia and hyperoxia, with or without added anti-Wnt5A neutralizing antibody (ab), recombinant Wnt5a, or IgG isotype control. Scale bars, 100 μm. (*B*) Airspace volume density (%) of PCLS cultured in normoxia relative to hyperoxia. $^{****}P < 0.0001$ by Welch's *t* test. (*C*) Mean linear intercept of PCLS cultured in normoxia and hyperoxia, with and without anti-Wnt5A antibody and with and without recombinant Wnt5A.$^{****}P < 0.0001$, $^{***}P < 0.001$, and $^{*}P < 0.05$ by two-way ANOVA and secondary analysis by Tukey's test for multiple comparisons. (*D*) Immunofluorescence for mitotic marker Ki67 (green) and epithelial marker Nkx2.1 (red) shows increased proliferation in PCLS in both Nkx2.1 positive and negative cells cultured in hyperoxia. $^{**}P < 0.01$. Scale bars, 10 μm. Quantification of $Ki67^{+}$ cells was determined by counting 36 high powered fields per group (green arrows indicate $Ki67^{+}$ cells). Data are representative of ⩾3 biological replicates for each condition, with 4 technical replicates for histology. NS = nonsignificant.

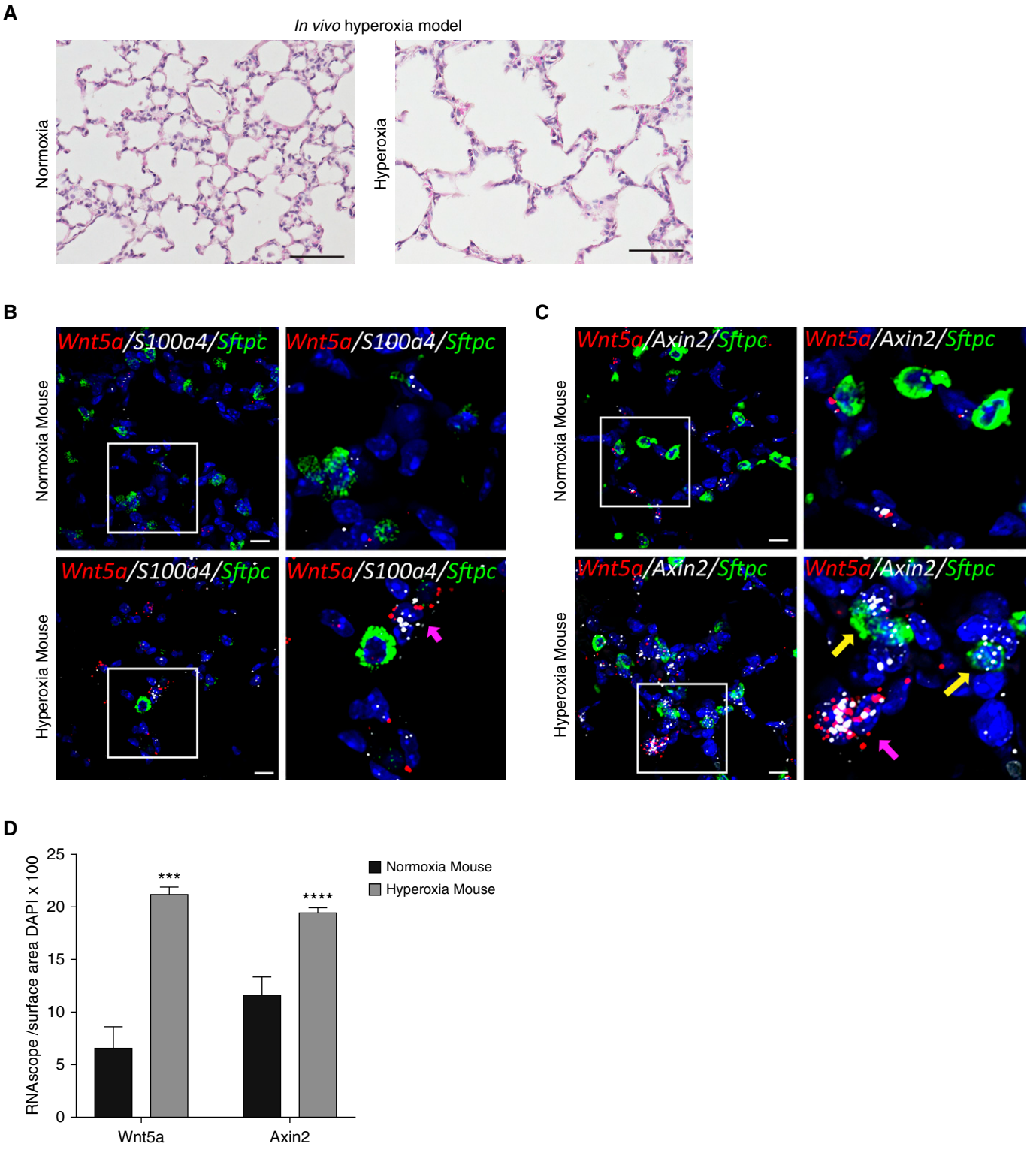

Figure 5. (*A*) Hematoxylin and eosin staining of neonatal mouse lungs after 14 days of exposure to normoxia or hyperoxia shows increased alveolar airspaces. Scale bars, 100 μm. (*B*) Multiplex RNA *in situ* hybridization (RNA ISH) showing increased expression of *Wnt5a* (red) coexpressed in cells also expressing fibroblast marker *S100a4* (white), with no expression of *Wnt5a* in cells expressing *Sftpc*; magenta arrow indicates cells coexpressing *S100a4* and *Wnt5a.* Scale bars, 10 μm. (*C*) Multiplex RNA ISH demonstrating expression of Wnt target gene *Axin2* in both *Wnt5A*-expressing cells (magenta arrow) and in adjacent *Sftpc*-expressing alveolar type 2 cells (yellow arrows). Scale bars, 10 μm. (*D*) Quantification of RNA ISH normalized to cell number shows significantly increased expression of both *Wnt5a* and *Axin2* in response to hyperoxia. ***$P < 0.001$ and ****$P < 0.0001$. White boxes in *B* and *C* denote area of inset. Data are representative of ⩾3 biological replicates for each condition, with 3 technical replicates for histology.

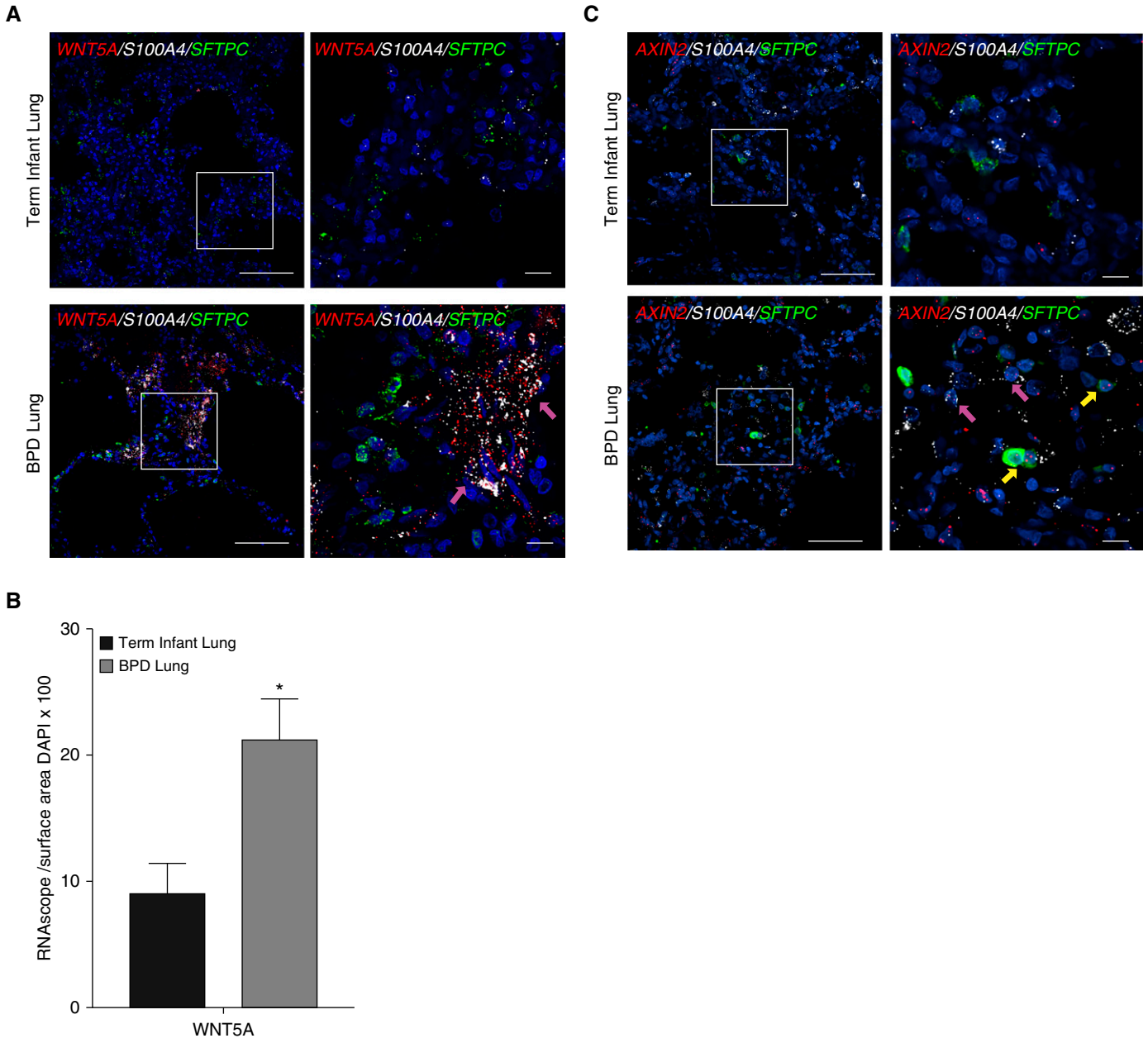

Figure 6. The pattern of mesenchymal expression of *WNT5A* is replicated in the lungs of human infants with bronchopulmonary dysplasia (BPD). (*A*) RNA *in situ* hybridization (RNA ISH) demonstrates increased expression of *WNT5A* (red) in lungs of infants who died with BPD (at >40 wk corrected gestational age at the time of death) when compared with term infants who died from nonrespiratory causes, with colocalization of *WNT5A* expression with expression of fibroblast marker *S100A4* (white) indicated by magenta arrows, and no expression of *WNT5A* in cells coexpressing *SFTPC*. Scale bars, 100 μm. (*B*) Quantification of RNA ISH normalized to nuclear surface area shows significantly increased expression of WNT5A by BPD lung tissue when compared with term infant controls. $^*P < 0.05$. (*C*) RNA ISH demonstrates increased expression of *AXIN2* (red) in cells coexpressing *S100A4* (magenta arrows) in lungs of infants who died with BPD (at >40 wk corrected gestational age at the time of death) when compared with term infants who died from nonrespiratory causes, with colocalization of *WNT5A* expression with expression of fibroblast marker *S100A4* (white) indicated by magenta arrows, and coexpression of *AXIN2* in cells coexpressing *SFTPC* (green) indicated by yellow arrows. Scale bars, 100 μm. White boxes in *A* and *C* denote inset area shown in higher magnification on the right. These data are representative of four infants who died with BPD at corrected gestational age 45–65 weeks and three term infant controls who died from nonrespiratory causes.

alone (Figures 7F and 7G and E5B). We observed no changes in Wnt5a expression after BAY11–7082 treatment in normoxia-exposed pups (Figure E5B).

To further investigate a requirement for NF-κB activation in driving *Wnt5A* expression in hyperoxia, fibroblasts were isolated from P2 lungs from double-transgenic mice that express a *Myc*-His–tagged mutant avian IκBα (dominant inhibitor of NF-κB activation) in a tet-on system (13) in which the reverse

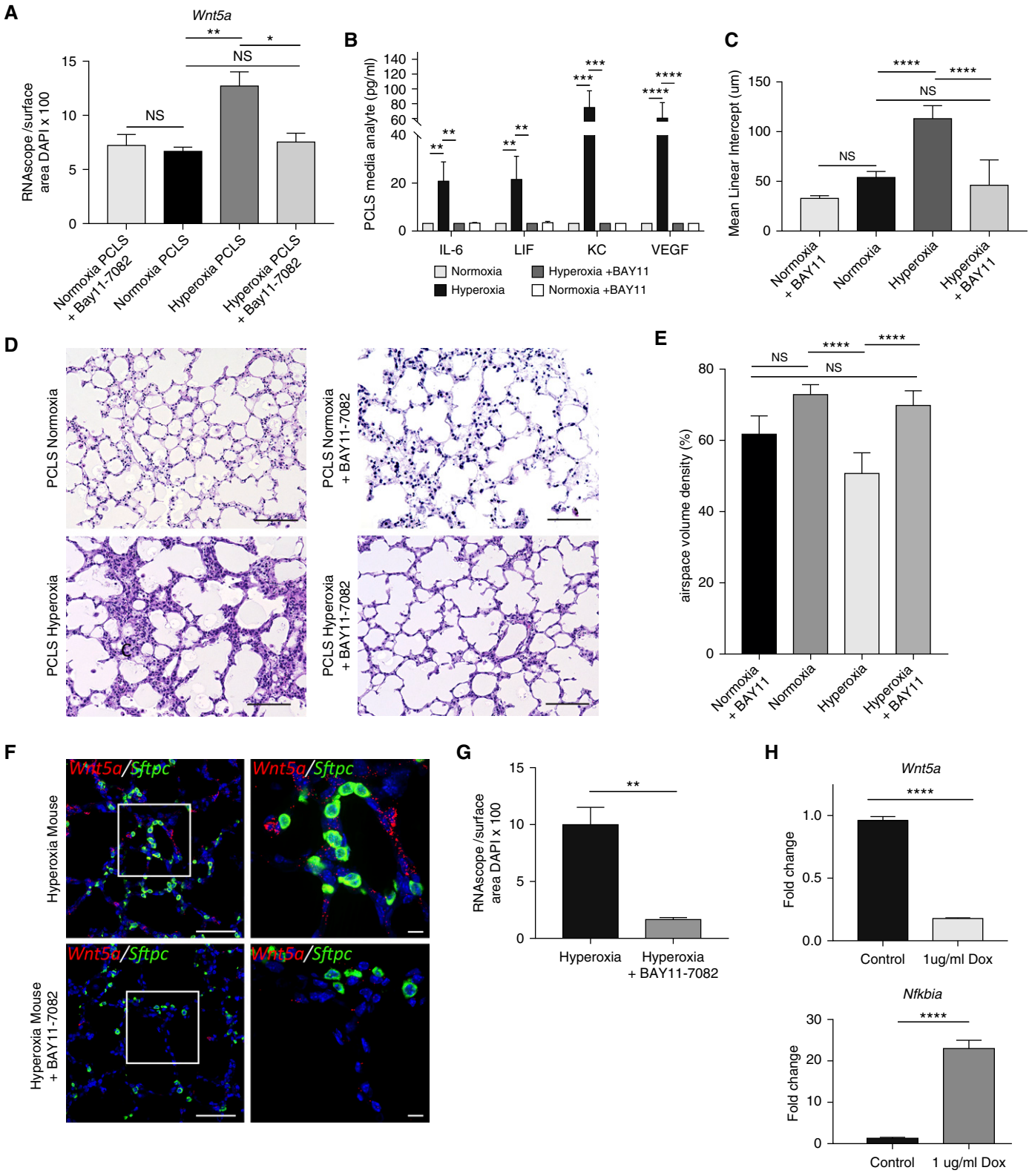

Figure 7. *Wnt5a* expression in the setting of hyperoxia injury is mediated by NF-κB (nuclear factor-κB) in the developing lung. (*A*) Quantification of *Wnt5a* expression normalized to cell number for each condition, analyzed by two-way ANOVA and secondary analysis by Tukey's test for multiple comparisons. $N = 4$, $^{*}P < 0.05$ and $^{**}P < 0.01$. (*B*) Cytokine analysis on tissue lysate samples from precision-cut lung slices (PCLS) from P4 lungs cultured in normoxia, hyperoxia, normoxia + BAY11–7082, and hyperoxia + BAY11–7082 ($n = 4$ mice per group). $^{**}P < 0.01$, $^{***}P < 0.001$, and $^{****}P < 0.0001$ by two-way ANOVA with secondary analysis by Tukey's test for multiple comparisons. (*C*) Mean linear intercept of PCLS cultured in normoxia or hyperoxia, with or

tetracycline transactivator is under control of the ubiquitous ROSA26 promoter (14). At passage 4, fibroblasts in culture were treated with doxycycline to induce transgene activation and expression of the dominant-negative IκBα, which resulted in significantly decreased *Wnt5a* expression under normoxia culture conditions (Figure 7H).

Inhibition of NF-κB signaling resulted in decreased expression of Wnt5A *in vitro, ex vivo*, and *in vivo*. Together, these data strongly suggest that in the setting of hyperoxia injury, NF-κB promotes mesenchymal expression of Wnt5A, and that upregulated Wnt5A mediates the impaired alveolarization and septal-thickening characteristic of BPD.

Discussion

Because Wnt/β-catenin signaling is present in both AT2 cells and fibroblasts in BPD tissues (6), we developed a human coculture system to study the contributions of both cell types to the Wnt signaling pathway and to the pathology of BPD. By focusing on the interactions between developing AT2 cells and fibroblasts after hyperoxia injury, we have established a BPD transcriptomic phenotype. Screening an array of Wnt ligands identified a critical mechanism that contributes to the BPD phenotype: dysregulated mesenchymal expression of Wnt5A. In addition, we demonstrated that the expression of Wnt5A by mesenchymal cells after hyperoxia injury can drive many features of the BPD phenotype *in vitro*, and this finding was replicated in the more complex *in vivo* and *ex vivo* mouse models. Further, we have found evidence of increased expression of Wnt5A in the lungs of infants who died with BPD relative to control subjects. Although dysregulated Wnt signaling is implicated in many lung diseases across the lifespan (5), the mechanism whereby lung injury results in aberrant Wnt signaling remains undefined. Building upon prior work that identified transcription factor binding sites for NF-κB in the Wnt5A promoter, we established a possible mechanism linking hyperoxia injury to Wnt5A exposure via increased NF-κB signaling, an inflammatory pathway well described as activated by hyperoxia injury. We found that chemical inhibition of NF-κB signaling *ex vivo* and *in vivo* and genetic inhibition of NF-κB signaling *in vitro* reduced *Wnt5a* expression, along with improved alveolarization in PCLS treated with an NF-κB inhibitor.

Although activated Wnt signaling is necessary for normal lung development, the timing and regulation of active Wnt signaling during development is tightly regulated (40, 41). In humans there is a peak of activated Wnt signaling in the lung at approximately 18 weeks gestation (3) and a second wave of Wnt signaling during alveologenesis (4), with very little active Wnt signaling present during the saccular stage (3, 7). Dysregulated activation of Wnt signaling (or a particular combination of Wnt ligands and receptors) during lung development appears to disrupt the normal developmental program of the lung. In this study, targeted inhibition of the Wnt5A ligand normalized lung development after hyperoxia injury in our model systems. Our findings are consistent with previous work in developmental lung biology using transgenic mice, which revealed that deletion of Wnt5A resulted in excessive distal airway branching, whereas overexpression of *Wnt5a* by epithelial cells inhibited lung development with decreased airway branching and dilatation of the distal airways (42, 43). Together, available data support our hypothesis that the overexpression of the Wnt pathway after injury in the developing lung results in the abnormal lung development that defines BPD.

Although Wnt5A has historically been described as acting in the noncanonical Wnt pathway, there is a growing realization that Wnt5A can act either canonically or noncanonically depending on the subtype of the Wnt receptor (33). In our dataset, we found evidence of canonical Wnt signaling with Wnt5A activation (e.g., increased accumulation of nuclear β-catenin and increased expression of the Wnt target gene *AXIN2*). Although Wnt5A was the Wnt ligand with the greatest increase in expression on our pathway array, other expression of other Wnt ligands was also altered by hyperoxia. With the diversity of Wnt ligands and receptors in the lung, it is possible that these and other ligands (or ligand and receptor combinations) are also contributing to the dysregulated Wnt signaling after saccular-stage hyperoxia exposure. While our human 3D-OTC used primary human AT2 and fibroblasts, a limitation of our mouse–human cocultures to determine the source of Wnt5A ligand is that the MLE-15 cells are derived from adult mice. Future work is necessary to identify the cell populations expressing these other Wnt ligands and to characterize their role in lung development and hyperoxia injury.

To determine if the increased *WNT5A* expression we observed in our human 3D-OTC model was relevant to the impaired alveolarization that defines BPD, we cultivated an *ex vivo* injury model using PCLS. An advantage of this system is that it allows for the manipulation of the lung with small molecules, without having to consider the side-effects and off-target effects of these small molecules on other organs in the mouse. PCLS also contains all of the resident cell types of the lung. The PCLS hyperoxia model in this study demonstrates the hallmark features of severe BPD with both alveolar simplification and septal thickening, with Wnt5A inhibition attenuating both components of the phenotype. In the future, this PCLS model could be adapted to examine less severe hyperoxic injury by

Figure 7. (*Continued*). without BAY11–7082, analyzed by two-way ANOVA and secondary analysis by Tukey's test for multiple comparisons. ****$P < 0.0001$. (*D*) Hematoxylin and eosin staining of PCLS cultured in normoxia or hyperoxia, with or without BAY11–7082. Scale bars, 100 μm. (*E*) Airspace volume density of PCLS cultured in normoxia and hyperoxia, with or without BAY11–7082. ****$P < 0.0001$. (*F*) Multiplex RNA *in situ* hybridization comparing expression of *Wnt5A* (red) in hyperoxia-exposed pups treated with BAY11–7082 on P12–13 and untreated hyperoxia pups; *Sftpc* expression is in green. Scale bars, 10 μm. (*G*) Quantification of RNA *in situ* hybridization normalized to nuclear surface area shows significantly decreased expression of *Wnt5a* in hyperoxia-exposed pups treated with BAY11–7082 when compared with untreated hyperoxia controls. **$P < 0.01$. (*H*) Expression of inducible dominant-negative inhibitor (with doxycycline treatment) of NF-κB signaling in mouse lung fibroblasts showed decrease in *Wnt5a* expression by real-time quantitative PCR (qPCR) when NF-κB signaling was inhibited. ****$P < 0.0001$. qPCR confirmed expression of IκBα gene *Nfkbia* with treatment of doxycycline. ****$P < 0.0001$. Data are representative of ⩾4 biological replicates for each condition, with 3 technical replicates for histology and 4 replicates used for qPCR. Dox = treated with doxycycline; NS = nonsignificant ($P > 0.05$).

shortening the duration or amount of hyperoxia exposure, as both duration and degree of hyperoxia have been demonstrated to effect the phenotypic changes of impaired alveolarization and septal thickening (35).

Hyperoxia has been shown previously to initiate an inflammatory response in the developing lung by mediating the NF-κB signaling pathway (44), and activation of NF-κB signaling pathway in the absence of injury is sufficient to alter normal lung development (45). Analysis of conditioned media in our *ex vivo* model revealed evidence of downstream NF-κB signaling with the signature of elevated cytokines IL-6, LIC, KC, and VEGF. This, combined with previous work reporting putative transcription factor binding sites for NF-κB within the Wnt5A promoter (36) prompted us to investigate whether NF-κB activation might be a mechanism by which hyperoxia exposure results in increased *WNT5A* expression and increased Wnt activity. The data presented here provide evidence for a mechanistic link between hyperoxia and increased mesenchymal expression of Wnt5A via NF-κB signaling, although it is possible that the link between NF-κB and increased Wnt expression is indirect through induction of inflammatory or other NF-κB–dependent mediators. As the PCLS model does not include a circulating immune system, additional inflammatory factors may mediate hyperoxia injury *in vivo*.

Both NF-κB and Wnt are precisely coordinated developmental pathways that are essential for normal lung development (4, 18, 46). The cellular crosstalk within and between developmental pathways after injury is complex: in some injury contexts, NF-κB signaling has been shown to be protective (47), and it is possible that other pathways in concert with NF-κB also drive Wnt5A expression after hyperoxia (37). This complexity is amplified by the fact that the hyperoxia injury associated with preterm birth occurs during the vulnerable saccular developmental stage. Future work is needed to fully understand the interaction between the Wnt and NF-κB signaling pathways in the context of saccular-stage injury and to identify subpopulations of cells driving the crosstalk between these pathways.

Because the Wnt/β-catenin signaling pathway is critical for the development of multiple major organ systems, including the lung, the utility of attempting to target this pathway as a therapeutic strategy, particularly in the premature infant population at highest risk for developing BPD, remains controversial. Global inhibition of this pathway would be incompatible with normal development; however, through precise ligand targeting at specific time points identified by biomarker evaluation in blood or tracheal aspirates, it may be possible to inhibit pathologic features of dysregulated Wnt signaling, while preserving lung development and injury repair. Results from this study suggest that the precise timing and spatial coordination of Wnt signaling necessary for normal lung development is disrupted by hyperoxia exposure, resulting in aberrant secretion of Wnt5A, likely by alveolar mesenchymal cells. The development of a therapeutic approach to target Wnt5a specifically represents a potential strategy to restore the normal balance of developmental signaling pathways in the lungs of preterm infants to prevent or reverse BPD. ■

Author disclosures are available with the text of this article at www.atsjournals.org.

Acknowledgment: Experiments were performed in part through the use of the Vanderbilt University Cell Imaging Shared Resource (supported by NIH Grants CA68485, DK20593, DK58404, DK5963). The p-β-catenin-Y489 antibody developed by J. Balsamo and J. Lilien was obtained from the Developmental Studies Hybridoma Bank created by the National Institute of Child Health and Human Development of the NIH at the University of Iowa, Department of Biology. The authors are grateful to Michael Koval for thoughtful discussions and insights.

References

1. Baraldi E, Filippone M. Chronic lung disease after premature birth. *N Engl J Med* 2007;357:1946–1955.
2. Surate Solaligue DE, Rodríguez-Castillo JA, Ahlbrecht K, Morty RE. Recent advances in our understanding of the mechanisms of late lung development and bronchopulmonary dysplasia. *Am J Physiol Lung Cell Mol Physiol* 2017;313:L1101–L1153.
3. Zhang M, Shi J, Huang Y, Lai L. Expression of canonical WNT/β-CATENIN signaling components in the developing human lung. *BMC Dev Biol* 2012;12:21.
4. Frank DB, Peng T, Zepp JA, Snitow M, Vincent TL, Penkala IJ, *et al*. Emergence of a wave of Wnt signaling that regulates lung alveologenesis by controlling epithelial self-renewal and differentiation. *Cell Reports* 2016;17:2312–2325.
5. Baarsma HA, Königshoff M. *'WNT-er is coming':* WNT signalling in chronic lung diseases. *Thorax* 2017;72:746–759.
6. Sucre JM, Vijayaraj P, Aros CJ, Wilkinson D, Paul M, Dunn B, *et al*. Posttranslational modification of β-catenin is associated with pathogenic fibroblastic changes in bronchopulmonary dysplasia. *Am J Physiol Lung Cell Mol Physiol* 2017;312:L186–L195.
7. Sucre JMS, Deutsch GH, Jetter CS, Ambalavanan N, Benjamin JT, Gleaves LA, *et al*. A shared pattern of β-catenin activation in bronchopulmonary dysplasia and idiopathic pulmonary fibrosis. *Am J Pathol* 2018;188:853–862.
8. Sucre JMS, Jetter CS, Loomans H, Williams J, Plosa EJ, Benjamin JT, *et al*. Successful establishment of primary type II alveolar epithelium with 3D organotypic coculture. *Am J Respir Cell Mol Biol* 2018;59:158–166.
9. Sucre JRM, Anderson Z, Fensterheim B, Cutrone A, Jetter C, Guttentag S. Sharing progress in neonatology (SPIN). Presented at the 34th International Workshop on Surfactant Replacement. Jun 7–8, 2019, Parma, Italy.
10. Gonzales LW, Angampalli S, Guttentag SH, Beers MF, Feinstein SI, Matlapudi A, *et al*. Maintenance of differentiated function of the surfactant system in human fetal lung type II epithelial cells cultured on plastic. *Pediatr Pathol Mol Med* 2001;20:387–412.
11. Gonzales LW, Guttentag SH, Wade KC, Postle AD, Ballard PL. Differentiation of human pulmonary type II cells in vitro by glucocorticoid plus cAMP. *Am J Physiol Lung Cell Mol Physiol* 2002;283:L940–L951.
12. Wade KC, Guttentag SH, Gonzales LW, Maschhoff KL, Gonzales J, Kolla V, *et al*. Gene induction during differentiation of human pulmonary type II cells *in vitro*. *Am J Respir Cell Mol Biol* 2006;34:727–737.
13. Chen SM, Cheng DS, Williams BJ, Sherrill TP, Han W, Chont M, *et al*. The nuclear factor kappa-B pathway in airway epithelium regulates neutrophil recruitment and host defence following *Pseudomonas aeruginosa* infection. *Clin Exp Immunol* 2008;153:420–428.
14. Benjamin JT, van der Meer R, Im AM, Plosa EJ, Zaynagetdinov R, Burman A, *et al*. Epithelial-derived inflammation disrupts elastin assembly and alters saccular stage lung development. *Am J Pathol* 2016;186:1786–1800.
15. Atkuri KR, Herzenberg LA, Niemi AK, Cowan T, Herzenberg LA. Importance of culturing primary lymphocytes at physiological oxygen levels. *Proc Natl Acad Sci USA* 2007;104:4547–4552.
16. Ambalavanan N, Nicola T, Hagood J, Bulger A, Serra R, Murphy-Ullrich J, *et al*. Transforming growth factor-beta signaling mediates hypoxia-induced pulmonary arterial remodeling and inhibition of alveolar

development in newborn mouse lung. *Am J Physiol Lung Cell Mol Physiol* 2008;295:L86–L95.
17. Ramani M, Bradley WE, Dell'Italia LJ, Ambalavanan N. Early exposure to hyperoxia or hypoxia adversely impacts cardiopulmonary development. *Am J Respir Cell Mol Biol* 2015;52:594–602.
18. Alvira CM. Nuclear factor-kappa-B signaling in lung development and disease: one pathway, numerous functions. *Birth Defects Res A Clin Mol Teratol* 2014;100:202–216.
19. Alsafadi HN, Staab-Weijnitz CA, Lehmann M, Lindner M, Peschel B, Königshoff M, *et al*. An *ex vivo* model to induce early fibrosis-like changes in human precision-cut lung slices. *Am J Physiol Lung Cell Mol Physiol* 2017;312:L896–L902.
20. Uhl FE, Vierkotten S, Wagner DE, Burgstaller G, Costa R, Koch I, *et al*. Preclinical validation and imaging of Wnt-induced repair in human 3D lung tissue cultures. *Eur Respir J* 2015;46:1150–1166.
21. Martin-Medina A, Lehmann M, Burgy O, Hermann S, Baarsma HA, Wagner DE, *et al*. Increased extracellular vesicles mediate WNT5A signaling in idiopathic pulmonary fibrosis. *Am J Respir Crit Care Med* 2018;198:1527–1538.
22. Paul MK, Bisht B, Darmawan DO, Chiou R, Ha VL, Wallace WD, *et al*. Dynamic changes in intracellular ROS levels regulate airway basal stem cell homeostasis through Nrf2-dependent Notch signaling. *Cell Stem Cell* 2014;15:199–214.
23. Wilkinson DC, Alva-Ornelas JA, Sucre JM, Vijayaraj P, Durra A, Richardson W, *et al*. Development of a three-dimensional bioengineering technology to generate lung tissue for personalized disease modeling. *Stem Cells Transl Med* 2017;6:622–633.
24. Wang F, Flanagan J, Su N, Wang LC, Bui S, Nielson A, *et al*. RNAscope: a novel *in situ* RNA analysis platform for formalin-fixed, paraffin-embedded tissues. *J Mol Diagn* 2012;14:22–29.
25. Plosa EJ, Young LR, Gulleman PM, Polosukhin VV, Zaynagetdinov R, Benjamin JT, *et al*. Epithelial β1 integrin is required for lung branching morphogenesis and alveolarization. *Development* 2014;141: 4751–4762.
26. Oh IH, Reddy EP. The myb gene family in cell growth, differentiation and apoptosis. *Oncogene* 1999;18:3017–3033.
27. Kim IM, Ramakrishna S, Gusarova GA, Yoder HM, Costa RH, Kalinichenko VV. The forkhead box m1 transcription factor is essential for embryonic development of pulmonary vasculature. *J Biol Chem* 2005;280:22278–22286.
28. Kalin TV, Wang IC, Meliton L, Zhang Y, Wert SE, Ren X, *et al*. Forkhead Box m1 transcription factor is required for perinatal lung function. *Proc Natl Acad Sci USA* 2008;105:19330–19335.
29. Tan FE, Vladar EK, Ma L, Fuentealba LC, Hoh R, Espinoza FH, *et al*. Myb promotes centriole amplification and later steps of the multiciliogenesis program. *Development* 2013;140:4277–4286.
30. Sucre JM, Wilkinson D, Vijayaraj P, Paul M, Dunn B, Alva-Ornelas JA, *et al*. A three-dimensional human model of the fibroblast activation that accompanies bronchopulmonary dysplasia identifies Notch-mediated pathophysiology. *Am J Physiol Lung Cell Mol Physiol* 2016;310:L889–L898.
31. Bruno MD, Bohinski RJ, Huelsman KM, Whitsett JA, Korfhagen TR. Lung cell-specific expression of the murine surfactant protein A (SP-A) gene is mediated by interactions between the SP-A promoter and thyroid transcription factor-1. *J Biol Chem* 1995;270:6531–6536.
32. Baarsma HA, Skronska-Wasek W, Mutze K, Ciolek F, Wagner DE, John-Schuster G, *et al*. Noncanonical WNT-5A signaling impairs endogenous lung repair in COPD. *J Exp Med* 2017;214:143–163.
33. Mikels AJ, Nusse R. Purified Wnt5a protein activates or inhibits beta-catenin-TCF signaling depending on receptor context. *PLoS Biol* 2006;4:e115.
34. Jobe AH. Animal models, learning lessons to prevent and treat neonatal chronic lung disease. *Front Med (Lausanne)* 2015;2:49.
35. Nardiello C, Mižíková I, Silva DM, Ruiz-Camp J, Mayer K, Vadász I, *et al*. Standardisation of oxygen exposure in the development of mouse models for bronchopulmonary dysplasia. *Dis Model Mech* 2017;10:185–196.
36. Katula KS, Joyner-Powell NB, Hsu CC, Kuk A. Differential regulation of the mouse and human Wnt5a alternative promoters A and B. *DNA Cell Biol* 2012;31:1585–1597.
37. Katoh M, Katoh M. Transcriptional mechanisms of WNT5A based on NF-kappaB, Hedgehog, TGFbeta, and Notch signaling cascades. *Int J Mol Med* 2009;23:763–769.
38. McLoed AG, Sherrill TP, Cheng DS, Han W, Saxon JA, Gleaves LA, *et al*. Neutrophil-derived IL-1β impairs the efficacy of NF-κB inhibitors against lung cancer. *Cell Reports* 2016;16:120–132.
39. Melisi D, Chiao PJ. NF-kappa B as a target for cancer therapy. *Expert Opin Ther Targets* 2007;11:133–144.
40. Warburton D, El-Hashash A, Carraro G, Tiozzo C, Sala F, Rogers O, *et al*. Lung organogenesis. *Curr Top Dev Biol* 2010;90:73–158.
41. Herriges M, Morrisey EE. Lung development: orchestrating the generation and regeneration of a complex organ. *Development* 2014;141:502–513.
42. Li C, Xiao J, Hormi K, Borok Z, Minoo P. Wnt5a participates in distal lung morphogenesis. *Dev Biol* 2002;248:68–81.
43. Li C, Hu L, Xiao J, Chen H, Li JT, Bellusci S, *et al*. Wnt5a regulates Shh and Fgf10 signaling during lung development. *Dev Biol* 2005;287: 86–97.
44. Michiels C, Minet E, Mottet D, Raes M. Regulation of gene expression by oxygen: NF-kappaB and HIF-1, two extremes. *Free Radic Biol Med* 2002;33:1231–1242.
45. Benjamin JT, Carver BJ, Plosa EJ, Yamamoto Y, Miller JD, Liu JH, *et al*. NF-kappaB activation limits airway branching through inhibition of Sp1-mediated fibroblast growth factor-10 expression. *J Immunol* 2010;185:4896–4903.
46. Iosef C, Alastalo TP, Hou Y, Chen C, Adams ES, Lyu SC, *et al*. Inhibiting NF-κB in the developing lung disrupts angiogenesis and alveolarization. *Am J Physiol Lung Cell Mol Physiol* 2012;302: L1023–L1036.
47. Alvira CM, Abate A, Yang G, Dennery PA, Rabinovitch M. Nuclear factor-kappaB activation in neonatal mouse lung protects against lipopolysaccharide-induced inflammation. *Am J Respir Crit Care Med* 2007;175:805–815.